




A Prospective Observational Study of Diagnostic Reliability of Semiquantitative and Quantitative High b-Value Diffusion-Weighted MRI in Distinguishing between Benign and Malignant Lung Lesions at 3 Tesla

Sudipta Mohakud¹  Rasmibala Das¹ Nerbadyswari D. Bag¹ Prasanta R. Mohapatra²
Pritinanda Mishra³ Suprava Naik¹

¹Department of Radiodiagnosis, All India Institute of Medical Sciences, Bhubaneswar, Odisha, India

²Department of Pulmonary Medicine and Critical Care, All India Institute of Medical Sciences, Bhubaneswar, Odisha, India

³Department of Pathology and Lab Medicine, All India Institute of Medical Sciences, Bhubaneswar, Odisha, India

Address for correspondence Sudipta Mohakud, MD, Department of Radiodiagnosis, All India Institute of Medical Sciences, Bhubaneswar 751019, Odisha, India (e-mail: drsudipta.m@gmail.com).

Indian J Radiol Imaging 2024;34:6–15.

Abstract

Aim The aim of this study was to evaluate the usefulness of high b-value diffusion-weighted imaging (DWI) to differentiate benign and malignant lung lesions in 3 Tesla magnetic resonance imaging (MRI).

Materials and Methods Thirty-one patients with lung lesions underwent a high b-value ($b = 1000 \text{ s/mm}^2$) DW MRI in 3 Tesla. Thirty lesions were biopsied, followed by histopathological analysis, and one was serially followed up for 2 years. Statistical analysis was done to calculate the sensitivity, specificity, and accuracy of different DWI parameters in distinguishing benign and malignant lesions. Receiver operating characteristic (ROC) curves were used to determine the cutoff values of different parameters.

Results The qualitative assessment of signal intensity on DWI based on a 5-point rank scale had a mean score of 2.71 ± 0.75 for benign and 3.75 ± 0.60 for malignant lesions. With a cutoff of 3.5, the sensitivity, specificity, and accuracy were 75, 86, and 77.6%, respectively. The mean ADC_{min} (minimum apparent diffusion coefficient) value of benign and malignant lesions was $1.49 \pm 0.38 \times 10^{-3} \text{ mm}^2/\text{s}$ and $1.11 \pm 0.20 \times 10^{-3} \text{ mm}^2/\text{s}$, respectively. ROC curve analysis showed a cutoff value of $1.03 \times 10^{-3} \text{ mm}^2/\text{s}$; the sensitivity, specificity, and accuracy were 87.5, 71.4, and 83.3%, respectively. For lesion to spinal cord ratio and lesion to spinal cord ADC ratio with a cutoff value of 1.08 and 1.38, the sensitivity, specificity, and accuracy were 83.3 and 87.5%, 71.4 and 71.4%, and 80.6 and 83.8%, respectively. The exponential ADC showed a low accuracy rate.

Conclusion The semiquantitative and quantitative parameters of high b-value DW 3 Tesla MRI can differentiate benign from malignant lesions with high accuracy and make it a reliable nonionizing modality for characterizing lung lesions.

Keywords

- ▶ magnetic resonance imaging
- ▶ diffusion-weighted imaging
- ▶ lung neoplasm

article published online
August 16, 2023

DOI <https://doi.org/10.1055/s-0043-1771530>.
ISSN 0971-3026.

© 2023. Indian Radiological Association. All rights reserved.
This is an open access article published by Thieme under the terms of the Creative Commons Attribution-NonDerivative-NonCommercial-License, permitting copying and reproduction so long as the original work is given appropriate credit. Contents may not be used for commercial purposes, or adapted, remixed, transformed or built upon. (<https://creativecommons.org/licenses/by-nc-nd/4.0/>)
Thieme Medical and Scientific Publishers Pvt. Ltd., A-12, 2nd Floor, Sector 2, Noida-201301 UP, India

Introduction

Lung cancer remains the leading cause of cancer incidence and mortality, with 2.1 million new lung cancer cases and 1.8 million deaths, representing close to one in five (18.4%) cancer deaths.¹

Early detection and characterization of lung lesions into benign and malignant are of great importance for further workup and treatment plans. Chest radiographs and computed tomography (CT) scans are primary modalities for morphological evaluation. In contrast, positron emission tomography (PET) CT is the modality for the functional evaluation of lung lesions, which uses ionizing radiation.

Diffusion-weighted imaging (DWI) is functional imaging used to detect the restricted diffusion of the water molecule in the body. Although its use is well established in the brain and very extensively investigated in the prostate and breast, there are few lung studies. There is insufficient data regarding advanced 3 Tesla magnetic resonance imaging (MRI) scanners for lung lesion characterization.^{2,3} The use of higher b-values (8,00–1,000 s/mm²) reduces the perfusion effect and increases the diffusion effect at the cost of SNR (signal-to-noise ratio) and with an increase in acquisition time.⁴

Hence, the primary purpose of our study was to evaluate the utility of high b-value (1000 s/mm², with reasonable SNR) DWI in the characterization of lung lesions in an advanced 3 Tesla MRI scanner using qualitative, semiquantitative, and quantitative parameters.

Materials and Methods

The study was designed as a prospective observational study and conducted in the department of radiology of a tertiary teaching hospital in Eastern India after obtaining clearance from the institutional ethics committee. The study was conducted from July 2019 to May 2021.

Patients aged more than 18 years with lung mass/nodule more than or equal to 1 cm detected by CT or chest radiograph were

included in our study after obtaining informed consent. The rationale behind the 1 cm size is that this is the minimum size advised for a CT-guided biopsy to avoid a biopsy diagnostic failure.

Proven lung cancer cases on treatment, patients with contraindications to MRI like non-MR compatible implants, patients who did not want to undergo MRI, and a definitive benign lesion in CT not requiring histopathological diagnosis like popcorn calcification in hamartoma were excluded.

Patients underwent lung MRI in a 70 cm bore-sized, 3 Tesla whole-body MR unit (Discovery, GE Healthcare, United States) with a maximum gradient strength of 45 mT/m and a slew rate of 200T/m/s, field of view of 50 cm using a 3.0 T GEM anterior array coil in the supine position.

The technical specifications for the imaging protocols of MRI are outlined in ►Table 1.

The DW images with b-value of 1,000 s/mm² were evaluated by two radiologists with more than 6 years of experience. The apparent diffusion coefficient (ADC) maps were generated using the combined 50, 800, and 1,000 s/mm² b values. On the DWI, a visually assessed 5-point score was given. A score of 1 indicates nearly no signal intensity (SI). Score 2: SI between 1 and 3. Score 3 indicates that the SI of the lesion was almost equal to the spinal cord. Score 4 represented the lesion with SI higher than the spinal cord. Lesions with a score of 5 had SI much higher than that of the spinal cord in the same section. After lesion localization on T2 WI (T2-weighted imaging) or T2 fat-suppressed imaging, manual region of interest (ROI) was drawn on the DWI image in the visually assessed most restricted area (darkest area on the ADC map corresponding to bright area on DWI), then cloned to all the series that included ADC and exponential ADC (eADC) maps (►Figs. 1–4). The minimum ADC value (average value minus standard deviation) within the ROI on the ADC map was the ADC min. However, the ROI size was variable for each case and dependent on the area of diffusion restriction. Another ROI was placed in the spinal canal on the DWI in the same slice and cloned to the ADC map to obtain the spinal

Table 1 The technical specifications for the imaging protocols of MRI

<p>1. T2W imaging:</p> <p>a) T2W Coronal: SSFSE BH</p> <ul style="list-style-type: none"> • TR: 2558. 4ms, TE: 90ms, Slice thickness: 4 mm, Slice gap: 0. 5, NEX: 1, Matrix: 288 × 384 • Pixel size: 1.0 × 1.4, Acceleration factor PE: 2 <p>b) T2W Axial: SSFSE BH</p> <ul style="list-style-type: none"> • TR: 2500. 0, TE: 90. 0, Slice thickness: 4mm, Slice gap: 0.5mm, NEX: 1, Matrix: 288 × 384 • Pixel size: 1.0 × 1.3, Acceleration factor: 2, Intensity correction: SCIC (Surface Coil Intensity Correction) <p>c) T2WI Axial FS: SSFSE BH FS</p> <ul style="list-style-type: none"> • TR: 2500. 0, TE: 90. 0, Slice thickness: 4mm, Slice gap: 0. 5mm, NEX:1, Matrix: 320 × 256 • Pixel size:1. 2 × 1. 5, Acceleration factor: 2, Intensity correction: SCIC
<p>2. T1W imaging:</p> <p>T1W axial: FSPGR BH</p> <ul style="list-style-type: none"> • TR:180, TE:2. 1/Fr, Flip angle:80, Slice thickness:4mm, Slice gap:0. 5mm, NEX:1, Matrix:320 × 256 • Pixel size:1. 2 × 2. 6, Acceleration factor:1. 5, Intensity correction: SCIC
<p>3. Diffusion-weighted imaging</p> <ul style="list-style-type: none"> • TR: 6000, TE: 66. 3/FE, Slice thickness: 4mm, Slice spacing: 1, NEX:1, Matrix: 96 × 128 • Pixel size: 4. 4 × 3. 3, Acceleration factor:1 • b-value- 50, 800, 1000 s/mm²

Abbreviations: BH, breath hold; FSPGR, fast spoiled gradient echo; NEX, number of excitations; MRI, magnetic resonance imaging; SCIC, Surface Coil Intensity Correction; SSFSE, single shot fast spin echo; T1W, T1-weighted; TE, time to echo; TR, repetition time.

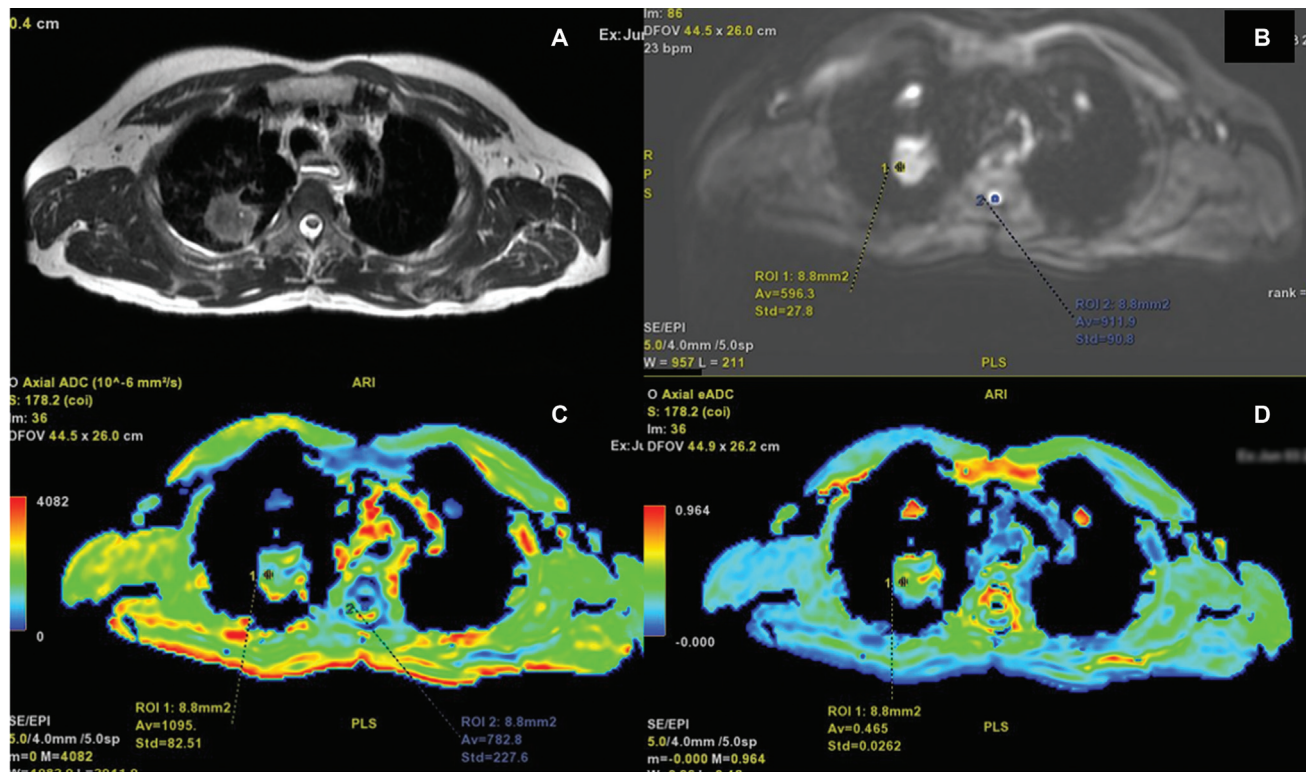


Fig. 1 The magnetic resonance imaging of a 51-year-old male patient who presented with a cough showing a single T2 hyperintense lesion (A) with an irregular margin located in the apical segment of the right upper lobe. The lesion showing diffusion restriction with a high lesion to spinal cord ratio value (B), lower minimum exponential apparent diffusion coefficient, and low lesion to spinal cord apparent diffusion coefficient ratio values (C). The measurement of the exponential apparent diffusion coefficient value (D) is shown. The histopathological diagnosis of the biopsy specimen was adenocarcinoma.

cord's SI and ADC values, respectively. Then lesion to spinal cord ratio (LSR), the SI ratio of the lesion and the spinal cord, was calculated. The eADC value was obtained. A ratio of the ADC_{min} value of the lesion and spinal cord was also calculated and represented as lesion to spinal cord ADC ratio (LSAR).

The patients underwent a biopsy under CT guidance for histopathological analysis. The patients who refused biopsy or lesions that appeared benign on imaging were serially followed up on imaging at 6 months, 1 year, 18 months, and 2 years if the size remained stable.⁵

The sample size was planned at 31 patients. Data analysis was done with the help of SPSS version 20.0 software (IBM Corporation, Armonk, New York, USA). Qualitative data were presented with the help of frequency and percentages. The independent student *t*-test assessed the association among quantitative study parameters. The *p*-value of less than 0.05 was considered significant. Receiver operating characteristics (ROC) analysis was used to calculate the diagnostic capability of different DWI parameters by taking histopathological diagnosis as the gold standard. The cutoff value for each parameter was obtained from the ROC curve analysis.

Results

Thirty-one patients (age range: 24–74 years; mean age 53.48 ± 11.54) with 31 lesions were scanned. There were 24 malignant (21 primary and 3 metastasis) and 7 benign lesions. In the malignant group, 21 out of 24 were male

patients, 15 were smokers (62.5%), and the rest were non-smokers. While in the benign group, only four patients were male, out of which two (28.5%) were smokers. The mean age of the malignant group was 54 years, and that of the benign group was 51.7 years. The most common clinical presentation of both benign and malignant groups was cough (100%), followed by weight loss (29%) and hemoptysis (25%). Other less common presentations were chest pain and breathlessness (<1%). The demographic features are described in **Table 2**. The mean diameter of malignant lesions ($n=24$) was 4.6 ± 1.8 cm, and that of benign lesions ($n=7$) was 5.3 ± 1.6 cm. Three out of 31 (9.7%) lesions had cavitation containing air. In 30 of 31 lesions, the final diagnosis was made histologically by CT-guided biopsy. The diagnosis of one benign lesion was made by a follow-up study that showed no change over 2 years. The histopathological diagnosis of the malignant and benign lesions with their mean diameter are compiled in **Table 3**.

DWI examinations were performed successfully, although respiratory ghosting artifacts caused image distortion; however, it was possible to obtain quantitative parameters for all lesions. The histopathology of the three cavitating lesions was abscess, squamous cell carcinoma (SCC), and adenocarcinoma.

The mean SI score of malignant lesions was (3.75 ± 0.60) significantly higher than that of benign lesions, which measured 2.71 ± 0.75 with a *p*-value of less than 0.05 on a 5-point rank scale on DWI. One malignant lesion scored 2, which was found to be adenocarcinoma, and 17 other malignant lesions

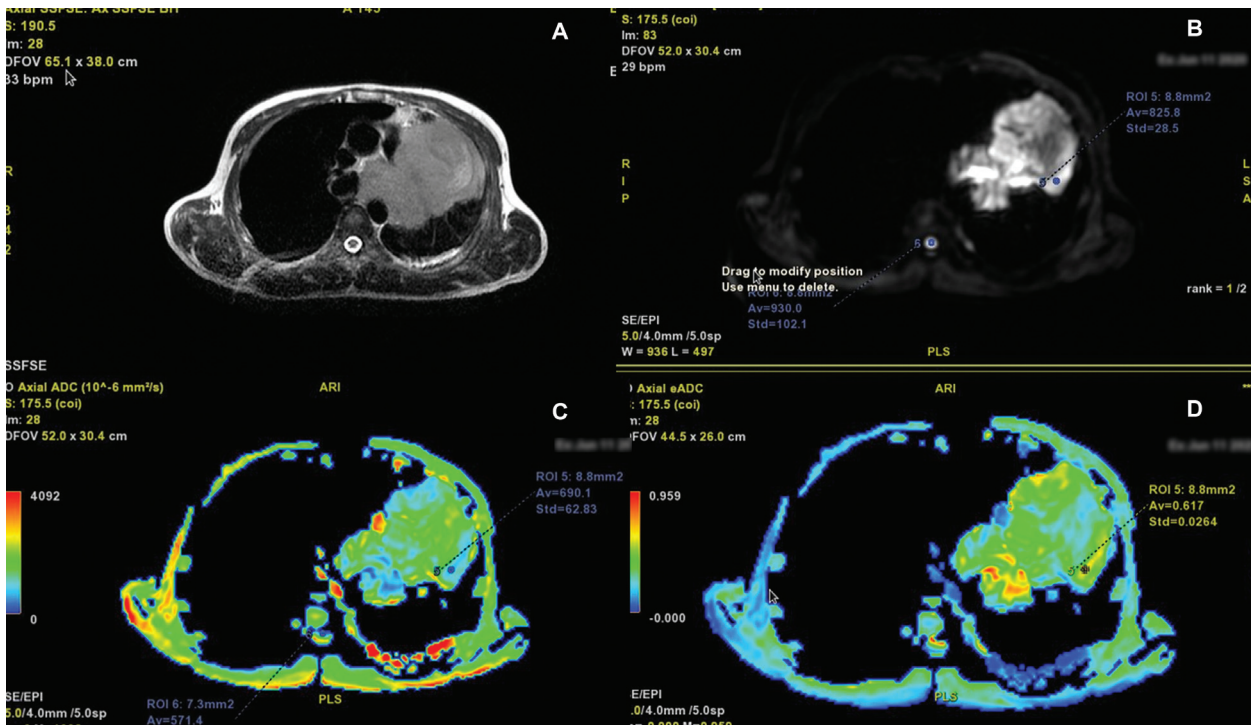


Fig. 2 The magnetic resonance imaging of a 38-year-old male smoker who presented with cough and weight loss showing a single T2 hyperintense lesion (A) with a lobulated margin in the apical segment of the left upper lobe. The lesion showing diffusion restriction with a high lesion to spinal cord ratio value (B), lower minimum apparent diffusion coefficient (ADC), and low lesion to spinal cord ADC ratio values (C). The measurement of the exponential ADC value (D) is shown. Associated features of mediastinal invasion and left pleural effusion are also seen. The histopathological diagnosis was small cell carcinoma.

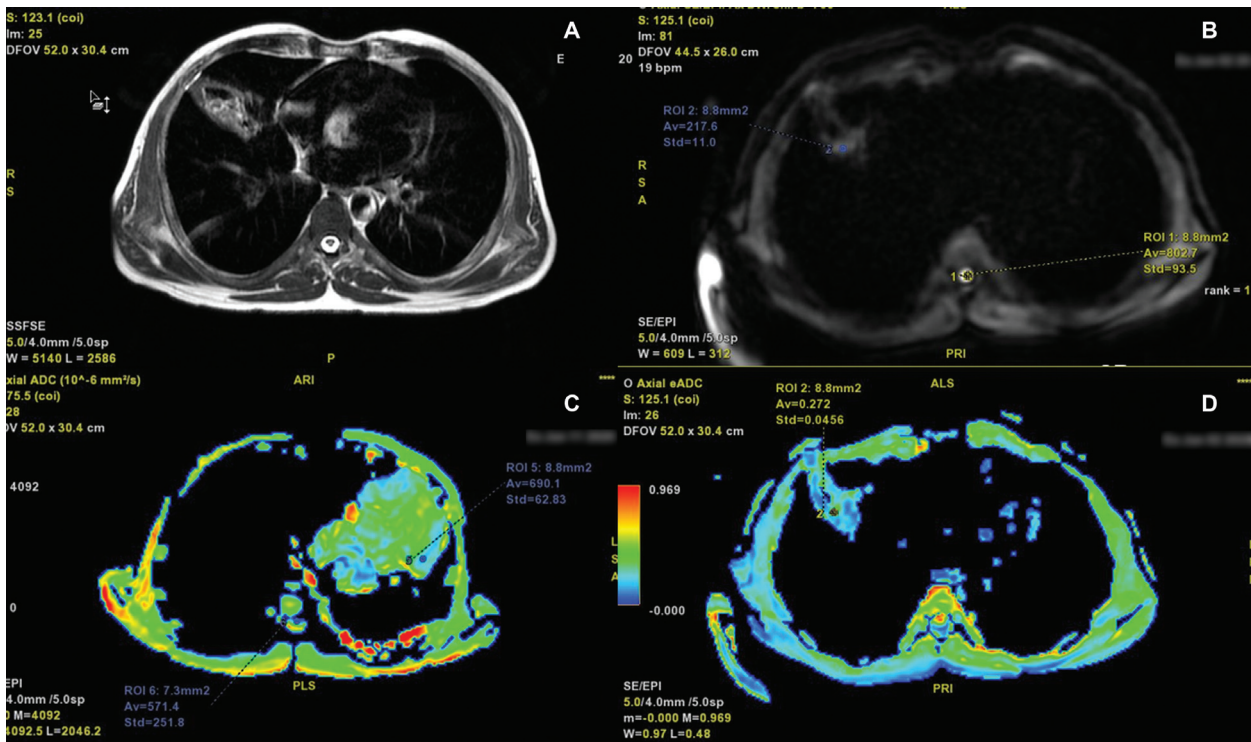


Fig. 3 The magnetic resonance imaging of a 51-year-old male with a cough not responding to medical treatment showing a solitary T2 hyperintense wedge-shaped lesion (A) with a smooth margin and internal cavitation in the right middle lobe. The lesion showing no significant diffusion restriction with a lower lesion to spinal cord ratio (B), higher minimum apparent diffusion coefficient (ADC), and higher lesion to spinal cord ADC ratio values (C). The measurement of the exponential ADC value (D) is shown. The histopathological diagnosis was granuloma, a benign lesion.

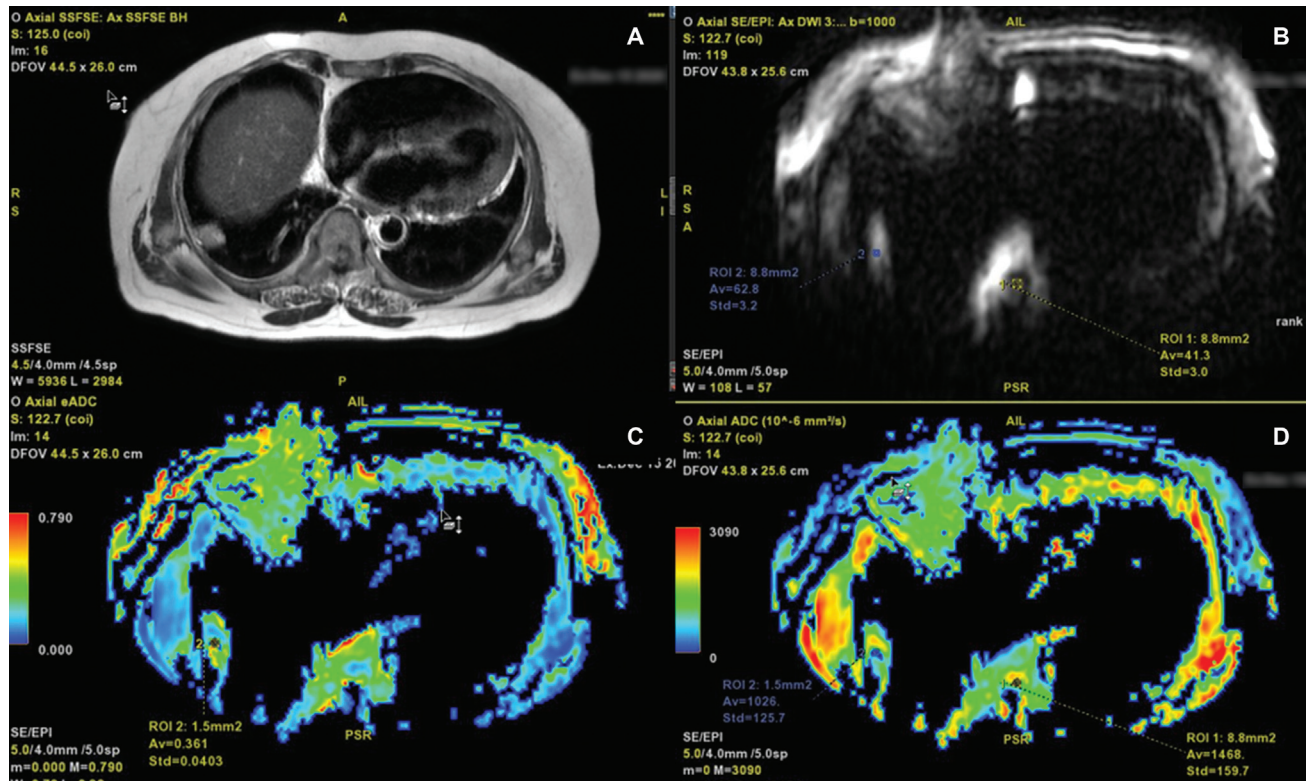


Fig. 4 The magnetic resonance imaging of a 65-year-old female with primary gastrointestinal malignancy showing a single peripheral T2 hyperintense (A) lesion with a lobulated margin in the right lower lobe. The lesion showing diffusion restriction with a high lesion to spinal cord ratio value (B). The exponential apparent diffusion coefficient (ADC) (C) map is also depicted. The low minimum ADC, and low lesion to spinal cord ADC ratio values (D) are noted. The histopathological diagnosis was a metastasis from a gastrointestinal tract primary.

Table 2 Comparison of demographic parameters among benign and malignant lesion groups

		Malignant (n = 24)	Benign (n = 7)
Smoking history	Smokers	15 (62.5%)	2 (28.5%)
	Nonsmokers	9 (37.5%)	5 (71.4%)
Age in years (mean ± SD)		54 ± 12.3	51.7 ± 8.5
Sex	Male	21 (87.5%)	4 (57.1%)
	Female	3 (12.5%)	3 (42.8%)

Abbreviation: SD, standard deviation.

Table 3 Histopathological patterns and their mean diameters

	Diagnosis	n = 31	Mean diameter
Malignant (n = 24)	Squamous cell carcinoma	3	6.8 ± 0.28
	Adenocarcinoma	13	4.12 ± 1.76
	Small cell carcinoma	1	8
	Metastasis	3	3.5 ± 0.83
	Poorly differentiated carcinoma	2	5.25 ± 1.62
	Others (adenosquamous carcinoma)	2	4.35 ± 0.77
Benign (n = 7)	Abscess	1	5.6
	Granuloma (tubercular)	2	5.75 ± 0.35
	Others (melioidosis, fungal pneumonia, Wegener's granulomatosis, and hamartoma)	4	5.1 ± 2.2

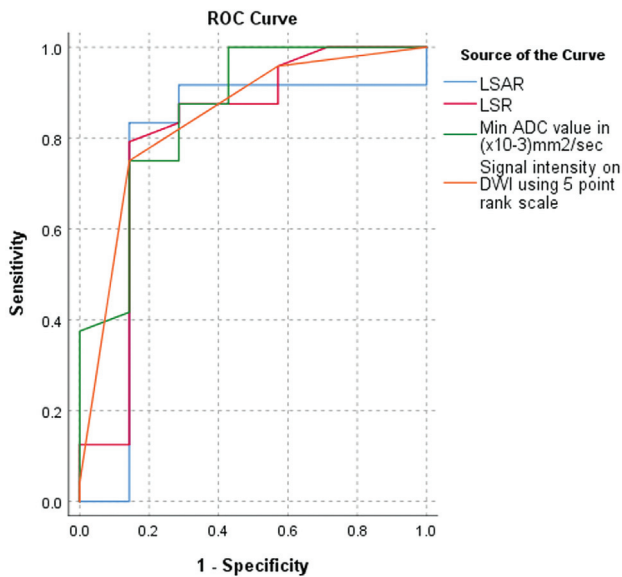


Fig. 5 Receiver operating characteristic (ROC) curve for 5-point rank scale on diffusion-weighted imaging (DWI) to differentiate benign and malignant lesions showing an area under the curve (AUC) as 0.842 (95% confidence interval [CI], 0.666–1.000). The AUC for minimum apparent diffusion coefficient (ADC) is 0.860 (95% CI, 0.691–1.000). The AUC for lesion to spinal cord ratio (LSR) on DWI to differentiate benign and malignant lesions is 0.810 (95% CI, 0.584–1.000). The AUC for lesion to spinal cord ADC ratio (LSAR) to differentiate benign and malignant lesions is 0.774 (95% CI, 0.520–1.000).

scored 4. One out of the seven benign lesions scored 4 that was a lung abscess. The area under the ROC curve (►Fig. 5) was 0.842 (95% confidence interval [CI], 0.666–1.000). With a threshold score of 3.5, the sensitivity, specificity, and accuracy were 75, 86, and 77.4%, respectively.

We obtained a weighted kappa value of 0.81 indicating an almost perfect interobserver agreement between the ADC_{min} values of the two radiologists with a standard error of 0.03 and 95% confidence interval. The ADC_{min} values were significantly lower in malignant lesions than in benign (*p*-value <0.05). The average ADC_{min} values (×10-3mm²/s) were 1.11 ± 0.38 for malignant lesion and 1.49 ± 0.38 for benign lesions (*p*-Value = <0.05). The mean LSR for malignant lesions was 1.23 ± 0.25 and for benign lesions was 0.94 ± 0.32 (*p*-value <0.05).

The area under the curve (AUC) for ADC_{min} was (0.860; 95% CI, 0.691–1.00) higher than that of LSR (0.801; 95% CI, 0.541–0.995; ►Fig. 5). The ROC curve analysis showed that

the optimum threshold for ADC_{min} and LSR to detect malignant lesions was 1.35 × 10-3mm²/s and 1.08, respectively. The sensitivity, specificity, and accuracy of ADC_{min} and LSR to differentiate benign and malignant lesions were calculated using these thresholds. The sensitivity of ADC_{min} (87.5%) was higher than LSR (83.3%). However, they had equal specificity of (71.4%) in differentiating benign and malignant lesions. ADC_{min} had a slightly better accuracy of 83.8% in correctly identifying the malignant and benign lesions than LSR, which had an accuracy of 80.6%. Highest LSR was found in poorly differentiated carcinoma.

Other diffusion parameters that were newly taken in this study include LSAR, which was calculated by dividing the ADC_{min} of the lesion by the ADC_{min} of the spinal cord in the same slice. A significant difference was also found for LSAR between benign and malignant lesions (*p*-value <0.05) with a mean value of 1.69 ± 0.82 and 1.09 ± 0.93, respectively. The ROC curve analysis of LSAR also showed fair results with an AUC of 0.774 (►Fig. 5). With an optimum cutoff value of 1.38, the sensitivity, specificity, and accuracy were similar to that of ADC_{min}, which were 87.5, 71.4, and 83.8%, respectively. Another parameter of DWI was eADC that showed very low AUC in ROC curve analysis with a low accuracy rate. No significant difference was found between benign and malignant lesions (*p*-Value >0.05) for eADC value. The mean value of different parameters in benign and malignant lesions is described in ►Table 4.

The subgroup analysis of DWI parameters between small cell carcinoma (SCLC) and non-small cell carcinoma (NSCLC) was done as represented in ►Table 5. Although we found mean ADC_{min} of SCC was lower than that of non-small cell carcinoma (NSCC), which correlates with the histopathological findings of high cellularity, high nuclear to the cytoplasmic ratio in SCC compared to NSCC; it was not statistically significant (*p*-Value =0.37). Similarly, we found higher mean LSR and lower mean LSAR values in SCC compared to NSCC (*p*-Value >0.05).

Discussion

Our prospective study used high b-value DW MRI to differentiate benign from malignant lung lesions using an advanced 3 Tesla scanner. We found that DWI can differentiate benign lung lesions from malignant ones with reasonable accuracy without using ionizing radiation as opposed to CT/PET. For the first time in our study, we used a new

Table 4 Comparison of mean values of different DW MRI parameters between benign and malignant lesions

Parameters	Benign lesions	Malignant lesions	p-Value
SI score	2.71 ± 0.75	3.75 ± 0.60	< 0.05
ADC _{min} (×10 ⁻³ mm ² /s)	1.49 ± 0.38	1.11 ± 0.20	< 0.05
LSR	0.94 ± 0.32	1.23 ± 0.25	< 0.05
LSAR	1.69 ± 0.82	1.09 ± 0.93	< 0.05
eADC	0.357 ± 0.15	0.389 ± 0.12	> 0.05

Abbreviations: eADC, exponential apparent diffusion coefficient; DW, diffusion-weighted; LSR, lesion to spinal cord ratio; LSAR, lesion to spinal cord ADC ratio; MRI, magnetic resonance imaging; SI, signal intensity.

Table 5 Comparison with previous studies for the evaluation of diagnostic capability of ADC value to diagnose malignant pulmonary lesions

Study	N/n (malignant/total)	b-Value (s/mm ²)	ADC ($\times 10^{-3}$ mm ² /s) Cutoff	Sensitivity (%)	Specificity (%)	Accuracy (%)
Present study	24/31	1,000	1.35	87.5	71.4	83.8
Uto et al ¹⁰	28/28	1,000	0.83	33	90	50
Çakır et al ⁹	46/48	1,000	1.5	86.7	88.9	–
Henz Concatto et al ¹²	49/49	800	1	83.3	93.5	89.8
Mori et al ²⁴	104/140	1,000	1.1	70	97	76
Das et al ²⁹	32/35	800	1.36	80	86.6	82.8

Abbreviation: ADC, apparent diffusion coefficient.

parameter, namely LSAR, that showed high specificity and sensitivity in the lesion characterization. Among the other DWI parameters, ADC_{min} and LSR also showed high positive predictive value for malignancy. However, the eADC value was statistically insignificant in distinguishing benign and malignant lesions.

DWI is a type of functional imaging that provides information on the molecular features that underlie pathological and physiological mechanisms.⁶ It is based on the diffusion of water molecules through the tissue of interest (tumors), the rate, and direction of that are closely related to the cell structure and integrity of cell membranes.⁷ Thus, the diffusion of water molecules is affected by many of the characteristic features of malignant tumors, including rapid cell proliferation, high cell density, large nuclei, high amounts of intracellular macromolecular proteins, high nuclear/cytoplasm ratio, and reduced extracellular space relative to normal tissue.^{6,7} Specifically, the diffusion of water molecules in malignant tumors is limited, resulting in a lower ADC value and facilitating the differentiation of malignant tumors from benign ones.

DWI can offer qualitative (visual assessment of the lesion), semiquantitative (LSR), and quantitative assessment (ADC measurement, LSAR, and eADC value measurement) of lung lesions.

In the qualitative method, a visual assessment of the lesion SI is compared to the spinal cord SI and scored based on a 5-point rank scale. In our study, the 5-point rank scale assessment had an area under the ROC curve of 0.842, which indicates a good test result. With an optimum cutoff value of 3.5, we found sensitivity, specificity, and accuracy of 75, 86, and 77.4%, respectively. Satoh et al and Çakır et al qualitatively assessed the lung lesion based on the 5-point scale of DWI and found that most malignant lesions are hyperintense compared to the spinal cord. With a score of 3 as a cutoff, Satoh et al found sensitivity and specificity of 89 and 61%, respectively. In contrast, Çakır et al found these values to be 93.3 and 88.9%, respectively, in differentiating benign from malignant lung lesions.^{8,9}

However, this qualitative assessment is subjective and observer-dependent. The semiquantitative evaluation method calculates the ratio of lesion SI to that of the spinal cord in the same slice to differentiate benign and malignant

lesions.¹⁰⁻¹² In our study, the LSR was significantly higher in malignant than benign lesions, with a *p*-value less than 0.05. The area under the ROC curve was 0.810. With a cutoff value of 1.08, we found an accuracy of 80.6%. Our study found a higher specificity than a study conducted by Satoh et al, who reported a sensitivity, specificity, and accuracy of 89, 61, and 89%, respectively.⁸ Henz Concatto et al and Uto et al used a cutoff value of 1.2 and 1.135, respectively. They found sensitivity, specificity, and accuracy of 88.8, 96.7, and 93.9% and 83, 90, and 86%, respectively.^{10,12} A meta-analysis by Shen et al reported that several studies that used LSR to differentiate benign and malignant lesions found sensitivity ranging from 73 to 97% and specificity ranging from 69 to 91%.⁴ Our study found similar results with a sensitivity and specificity of 83.3 and 71.4%, respectively. The difference between our study and previous studies was apparently because of different b values and external magnetic field magnitude, which was 3 Tesla in our case compared to 1.5 T in other studies.

Higher b-values reduce the perfusion effect and increase the diffusion effect. However, the SNR is adversely affected at higher b-values.¹³ Considering the b-values between 500 and 1000 s/mm² for body imaging, we used a b-value of 1000 s/mm² to get optimum SNR with a better diffusion effect. Higher b-values (800-1000 s/mm²) are advised with reasonable SNR, which can be achieved by taking multiple b-values with the expense of an increase in acquisition time.⁴

Quantitative assessment can also be done using DWI by calculating the ADC value. ADC measures the magnitude of water protons movement, which can be compromised by increased cellularity or density of malignant lesions. The intracellular structural alteration also contributes to the low ADC value in tumors. Studies by Uto et al and Wang et al showed no difference in ADC values between benign and malignant nodules.^{10,14} However, many other studies found that ADC values of carcinoma lungs are lower than benign lesions, which are also supported by our study.^{12,15} Studies conducted by Cui et al and Weller et al revealed good inter- and intraobserver variability of ADC values in DWI.^{16,17} Hence, ADC is a good and safe marker for the characterization of lung lesions. Çakır et al and Uto et al documented mean ADC values of 2.02×10^{-3} mm²/s, 1.15×10^{-3} mm²/s, and 1.19×10^{-3} mm²/s, 1.01×10^{-3} mm²/s for benign and

Table 6 Comparison of diagnostic capabilities of different DW-MRI parameters in distinguishing benign and malignant lesions

Parameters	AUC	Cutoff	Sensitivity (%)	Specificity (%)	Accuracy (%)	p-Value
SI score	0.842	3.5	75	86	77.4	0.007 (< 0.05)
ADC min ($\times 10^{-3}$ mm ² /s)	0.860	1.35	87.5	71.4	83.8	0.004 (< 0.05)
LSR	0.810	1.08	83.3	71.4	80.6	0.014 (< 0.05)
LSAR	0.774	1.38	87.5	71.4	83.8	0.030 (< 0.05)
eADC	0.518	0.282	87.5	42.9	74.19	0.88 (> 0.05)

Abbreviations: AUC, area under the curve; eADC, exponential apparent diffusion coefficient; DW, diffusion-weighted; LSR, lesion to spinal cord ratio; LSAR, lesion to spinal cord ADC ratio; MRI, magnetic resonance imaging; SI, signal intensity.

Table 7 Comparison of DWI parameters between small cell and non-small cell carcinoma group

Parameters	Small cell carcinoma	Non-small cell carcinoma	p-Value
ADC _{min} ($\times 10^{-3}$ mm ² /s)	0.84 \pm 0.09	1.15 \pm 0.18	0.37
LSR	1.37 \pm 0.02	1.25 \pm 0.23	0.07
LSAR	0.66 \pm 0.25	1.15 \pm 0.98	0.36

Abbreviations: ADC, exponential apparent diffusion coefficient; DWI, diffusion-weighted imaging; LSR, lesion to spinal cord ratio; LSAR, lesion to spinal cord ADC ratio.

malignant lesions, respectively.^{9,10} Gümüştas et al documented mean ADC values of 1.5×10^{-3} mm²/s and 1.9×10^{-3} mm²/s for malignant and benign lesions, respectively.¹⁸ Our study found a mean ADC_{min} value of 1.49×10^{-3} mm²/s for benign and 1.11×10^{-3} mm²/s for malignant lesions. The low ADC value of malignant lesions compared to benign lesions was also supported by Liu et al and Tondo et al.^{15,19}

The difference in the ADC values of our study from others can be attributed to the fact that we used ADC_{min}, while others used the mean ADC. The ADC_{min} value is more effective than the mean ADC value in distinguishing between malignant and benign tumors.^{20–22} Minimal changes in the diffusion restriction of the malignant lesion with significant cystic or necrotic components may cause marked ADC variation. However, ADC_{min} is the lowest ADC value in tissues. A study by Zhang et al also supported the highest diagnostic value of ADC_{min} in differentiating breast lesions.²³ The comparative analysis of the diagnostic accuracy of ADC values of various studies with our study is summarized in **Table 5**.

Among LSR and ADC_{min}, Çakmak et al found ADC_{min} was superior to LSR in differentiating benign and malignant lesions, while Koyama et al documented LSR as superior and convenient to ADC.^{11,13} Our study found ADC_{min} to have a slightly higher AUC of 0.860 than LSR (0.810) and slightly higher sensitivity and accuracy, similar to Çakmak et al study.¹³ The variations in the cutoff values may be because the studies are conducted at different magnetic field strengths (some in 1.5 T and some in 3 Tesla) and variable b-values and unstandardized ROI delineation. Newer DWI parameter like LSAR, defined as the ratio of ADC value of the lesion to that of the spinal cord, was evaluated for the first time in our study. LSAR was equally sensitive and specific to ADC_{min} in differentiating benign and malignant lesions.

However, another parameter, eADC, was statistically insignificant in distinguishing benign and malignant lesions.

Mori et al found that DWI had no significant difference in sensitivity and accuracy than PET in distinguishing benign and malignant pulmonary lesions. However, it was superior in specificity (97%) due to fewer false-positive diagnoses than PET (79%).²⁴

The diagnostic capabilities of DWI parameters in various studies are compared in **Table 6**.

The subgroup analysis of DWI parameters between SCLC and NSCC was done as represented in **Table 7**. The mean ADC_{min} of SCLC was lower than that of NSCC, which correlates with the histopathological findings of high cellularity and nuclear to the cytoplasmic ratio in SCLC compared to NSCLC. However, it was not statistically significant (p-value = 0.37). Similarly, we found higher mean LSR and lower mean LSAR values in SCLC than in NSCLC (p-value > 0.05). Koyama et al. found significantly low ADC_{min} in SCLC compared to NSCLC.²⁵

This discrepancy can be explained because they had not considered cavitory or air-containing lesions. However, in our study, we have included all kinds of lesions, some (3 out of 31 lesions) of which are cavitating. The presence of air causes susceptibility artifacts on DWI and might have affected the ADC values. In a different study by Koyama et al, subtype classification was limited because the ADC measurement was affected by susceptibility artifacts and magnetic field inhomogeneities.²⁶

To the best of our search, we did not find any research on the utility of eADC values in lung lesions. Researchers have found eADC values as an effective quantitative parameter with comparable sensitivity and specificity to the ADC values in differentiating benign from malignant lesions in the breast and renal tumors at 3 Tesla MRI.^{27,28} The eADC values were not effective in differentiating benign from malignant lung

lesions in our study. The quoted studies have used b-values of 500 to 800 s/mm², and they have conducted the study in the breast and renal tumors that do not have air surrounding them or air-containing cavities within them. So, the measurement of eADC values might have been affected due to susceptibility artifacts by air in our study. A higher b-value (1000 s/mm²) would have resulted in more magnetic field inhomogeneities affecting the measurement of eADC values. Further studies are required at 3 Tesla with b = 1000 s/mm² to comment on the usefulness of eADC value in lung lesion characterization.

The strengths of our study were that it was conducted in an advanced 3 Tesla MRI scanner with high resolution and both qualitative and quantitative parameters were used for lesion characterization. The major limitations were a small number of benign lesions, which can be attributable to fewer biopsies done for suspected benign lesions and patients not turning up for follow-up imaging, a small sample size, and a single-center study. Another limitation of the study was the inclusion of lesions with air-filled cavities that might generate artifactual values affecting the mean DWI and ADC values and the final cutoff values. Further studies with more benign lesions are advised in the future to see how it impacts the results. Further multicentric research can throw light on LSR, LSAR, and ADC_{min} as the potential MRI biomarkers for lung cancer.

Note

Informed patient consent was obtained before subjecting the patient to MRI lung.

Funding

None.

Conflict of Interest

None declared.

Acknowledgement

We would like to thank Mrs. Sumitra Ghadei, Mr. Himansu, Mr. Subodh, and Mr. Guruprasad for helping in conducting the MRIs, and Dr. Dinesh Prasad for helping in the statistical analysis.

References

- Bray F, Ferlay J, Soerjomataram I, Siegel RL, Torre LA, Jemal A. Global cancer statistics 2018: GLOBOCAN estimates of incidence and mortality worldwide for 36 cancers in 185 countries. *CA Cancer J Clin* 2018;68(06):394–424
- Chen L, Zhang J, Bao J, et al. Meta-analysis of diffusion-weighted MRI in the differential diagnosis of lung lesions. *J Magn Reson Imaging* 2013;37(06):1351–1358
- Tyagi N, Cloutier M, Zakian K, Deasy JO, Hunt M, Rimner A. Diffusion-weighted MRI of the lung at 3T evaluated using echo-planar-based and single-shot turbo spin-echo-based acquisition techniques for radiotherapy applications. *J Appl Clin Med Phys* 2019;20(01):284–292
- Shen G, Ma H, Liu B, Ren P, Kuang A. Diagnostic performance of DWI with multiple parameters for assessment and characterization of pulmonary lesions: a meta-analysis. *Am J Roentgenol* 2018;210(01):58–67
- Gould MK, Donington J, Lynch WR, et al. Evaluation of individuals with pulmonary nodules: when is it lung cancer? Diagnosis and management of lung cancer, 3rd ed: American College of Chest Physicians evidence-based clinical practice guidelines. *Chest* 2013;143(05):e93S–e120S
- Alnaghy EA, El-Nahas MA, Sadek AG, Gwely NN, Elrakhawy MM. Role of diffusion-weighted magnetic resonance imaging in the differentiation of benign and malignant pulmonary lesions. *Pol J Radiol* 2018;83:e569–e578
- Koh DM, Collins DJ. Diffusion-weighted MRI in the body: applications and challenges in oncology. *Am J Roentgenol* 2007;188(06):1622–1635
- Satoh S, Kitazume Y, Ohdama S, Kimura Y, Taura S, Endo Y. Can malignant and benign pulmonary nodules be differentiated with diffusion-weighted MRI? *Am J Roentgenol* 2008;191(02):464–470
- Çakır Ç, Gençhellaç H, Temizöz O, Polat A, Şengül E, Duygulu G. Diffusion weighted magnetic resonance imaging for the characterization of solitary pulmonary lesions. *Balkan Med J* 2015;32(04):403–409
- Uto T, Takehara Y, Nakamura Y, et al. Higher sensitivity and specificity for diffusion-weighted imaging of malignant lung lesions without apparent diffusion coefficient quantification. *Radiology* 2009;252(01):247–254
- Koyama H, Ohno Y, Seki S, et al. Value of diffusion-weighted MR imaging using various parameters for assessment and characterization of solitary pulmonary nodules. *Eur J Radiol* 2015;84(03):509–515
- Henz Concatto N, Watte G, Marchiori E, et al. Magnetic resonance imaging of pulmonary nodules: accuracy in a granulomatous disease-endemic region. *Eur Radiol* 2016;26(09):2915–2920
- Çakmak V, Ufuk F, Karabulut N. Diffusion-weighted MRI of pulmonary lesions: comparison of apparent diffusion coefficient and lesion-to-spinal cord signal intensity ratio in lesion characterization. *J Magn Reson Imaging* 2017;45(03):845–854
- Wang MJ, Zhang W, Zhang N. Diagnostic value of 3.0T magnetic resonance diffusion-weighted imaging in benign and malignant lung tumors. *Acta Acad Med Jiangxi*. 2011;51:14–19
- Liu H, Liu Y, Yu T, Ye N. Usefulness of diffusion-weighted MR imaging in the evaluation of pulmonary lesions. *Eur Radiol* 2010;20(04):807–815
- Cui L, Yin JB, Hu CH, Gong SC, Xu JF, Yang JS. Inter- and intra-observer agreement of ADC measurements of lung cancer in free breathing, breath-hold and respiratory triggered diffusion-weighted MRI. *Clin Imaging* 2016;40(05):892–896
- Weller A, Papoutsaki MV, Waterton JC, et al. Diffusion-weighted (DW) MRI in lung cancers: ADC test-retest repeatability. *Eur Radiol* 2017;27(11):4552–4562
- Gümüştas S, Inan N, Akansel G, Ciftçi E, Demirci A, Özkara SK. Differentiation of malignant and benign lung lesions with diffusion-weighted MR imaging. *Radiol Oncol* 2012;46(02):106–113
- Tondo F, Saponaro A, Stecco A, Lombardi M, Casadio C, Carriero A. Role of diffusion-weighted imaging in the differential diagnosis of benign and malignant lesions of the chest-mediastinum. *Radiol Med (Torino)* 2011;116(05):720–733
- Onishi N, Kanao S, Kataoka M, et al. Apparent diffusion coefficient as a potential surrogate marker for Ki-67 index in mucinous breast carcinoma. *J Magn Reson Imaging* 2015;41(03):610–615
- Bonarelli C, Teixeira PA, Hossu G, et al. Impact of ROI positioning and lesion morphology on apparent diffusion coefficient analysis for the differentiation between benign and malignant nonfatty soft-tissue lesions. *Am J Roentgenol* 2015;205(01):W106–13
- Karaman A, Durur-Subasi I, Alper F, et al. Correlation of diffusion MRI with the Ki-67 index in non-small cell lung cancer. *Radiol Oncol* 2015;49(03):250–255

- 23 Zhang W, Jin GQ, Liu JJ, et al. Diagnostic performance of ADCs in different ROIs for breast lesions. *Int J Clin Exp Med* 2015;8(08): 12096–12104
- 24 Mori T, Nomori H, Ikeda K, et al. Diffusion-weighted magnetic resonance imaging for diagnosing malignant pulmonary nodules/masses: comparison with positron emission tomography. *J Thorac Oncol* 2008;3(04):358–364
- 25 Koyama H, Ohno Y, Nishio M, et al. Diffusion-weighted imaging vs STIR turbo SE imaging: capability for quantitative differentiation of small-cell lung cancer from non-small-cell lung cancer. *Br J Radiol* 2014;87(1038):20130307
- 26 Koyama H, Ohno Y, Aoyama N, et al. Comparison of STIR turbo SE imaging and diffusion-weighted imaging of the lung: capability for detection and subtype classification of pulmonary adenocarcinomas. *Eur Radiol* 2010;20(04):790–800
- 27 Zhang YL, Yu BL, Ren J, et al. EADC values in diagnosis of renal lesions by 3.0 T diffusion-weighted magnetic resonance imaging: compared with the ADC values. *Appl Magn Reson* 2013;44(03): 349–363
- 28 Kothari S, Singh A, Das U, Sarkar DK, Datta C, Hazra A. Role of exponential apparent diffusion coefficient in characterizing breast lesions by 3.0. Tesla diffusion-weighted magnetic resonance imaging. *Indian J Radiol Imaging* 2017;27(02):229–236
- 29 Das SK, Yang DJ, Wang JL, Zhang C, Yang HF. Non-Gaussian diffusion imaging for malignant and benign pulmonary nodule differentiation: a preliminary study. *Acta Radiol* 2017;58(01):19–26